ORIGINAL CONTRIBUTION

Thermal Activated Adsorbent from *D. sissoo* Sawdust for Fluoride Removal: Batch Study

Saurabh Joshi[1] · Mansi Garg[1] · Somen Jana[1]

Abstract The paper represents Thermal Activated *D. sissoo* Saw Dust (TADS) bioadsorbent for fluoride removal from water. Conventional single parameter study showed TADS dose, time and temperature had positive effect on removal, whereas pH and fluoride concentration negatively affected the sorption process. The Langmuir isotherm demonstrated monolayer adsorption capacity as 0.7 mg fluoride/g while 1/n as 0.2 of Freundlich model confirmed that adsorption was favourable. Thermodynamic parameters showed endothermic nature of fluoride TADS interaction. The 2.9 pH_{zpc} correlated the optimum solution pH with charge distribution. SEM–EDS confirmed the sorption by highlighting the changes in TADS morphology. RSM-BBD (Box–Behnken design) was further executed to model fluoride removal process. It predicted 45% removal at solution pH 6.0, TADS dose 12.0 g/L, 8.0 mg/L fluoride, 90 min contact time and 25 °C temperature. ANN model was also constructed, and it predicted 37% removal at given parameters. Finally, regeneration of TADS was performed and evaluated to demonstrate successful economical application in fluoride removal.

Keywords *Dalbergia sissoo* saw dust · Fluoride · RSM · ANN · Isotherm · Regeneration

✉ Somen Jana
somenjana@banasthali.in

[1] Department of Chemical Engineering, Banasthali Vidyapith, Tonk, Rajasthan, India

Introduction

Water is the base of life on the earth, and sustainability of life depends on it. Fresh and clean water is required not only for the survival but also for leisure and societal growth. Although 70% of earth surface is covered by water, only 3% of total water is fresh water, while rest of the water is not drinkable. Out of the total fresh water, major part (around 2%) is present in polar ice, glacier, while less than 1% is available as groundwater, lakes and rivers. So, the groundwater, lakes and rivers are said to be the primary sources of fresh water which are suitable for consumption [1]. Surface water and groundwater dissolve various compounds in it which are the result of numerous natural and human activities. These constituents are either natural like dissolved oxygen, silica, fluoride, etc., or may be manmade like petrochemical derivatives and dyes. Suitability of water for above-said purposes depends on chemicals and physical parameters of water.

Fluorine is one of the natural contaminants that have affected population across the globe. It is the lightest halogen, abundant, highest electronegative and reactive element found in nature. Fluorine does not exist as element due to highly reactive nature and forms complexes with other elements which are known as fluorides. It exists either as inorganic like sodium fluoride (NaF) or organic fluoride like monofluoroacetic acid (FCH_2CO_2H), Teflon and CFC. While organic fluoride is less common, inorganic fluoride complexes such as fluorspar, cryolite, sellaite and fluorapatite are found to be dominant in the environment. These ores, minerals and rocks are the cause of the fluoride pollution in water. They come into the contact of surrounding water and release fluoride out into the water, and thus, fluoride content increases in water. Fluoride concentration in such aquifers ranges from 0.1 to 15 ppm due to above-said industrial

activities and also for natural activities [2]. Normally, low amount of fluoride (upto 1.5 ppm) is crucial for dental enamel formation and bone mineralization, which is the reason for the presence of fluoride in the toothpaste. These beneficial effects are mostly considered in early childhood during bone and dental formation. On the other hand, higher fluoride uptake leads to various adverse effects on overall physiology. These adverse effects can be characterized as acute and chronic one. Acute effects consider vomiting, nausea, headaches, coma, cardiac arrest and death. While chronic effects include deterioration bone-teeth structure and appearance (Dental and skeletal fluorosis), muscle weakness and pain, delay in fracture healing, bone volume reduction, infertility, cancer, Alzheimer, brain damage, damage to DNA, stomach irritation and kidney and thyroid disorder [3, 4].

Several investigators have used diverse practices to decrease fluoride concentration in potable water. Some approaches such as sorption, coagulation and precipitation, electrocoagulation, electrodialysis and membrane separation process are widely applied to achieve the objective. In adsorption, fluoride ion present in water is blocked on the exterior of solid adsorbent and get eliminated from the bulk of liquid. In the coagulation, specific chemical (i.e. coagulant) is mixed to the bulk liquid to produce heavy flocs which catches fluoride and settles. Electrocoagulation is another form of coagulation process to produce floc by the application of electricity. The membrane separation and electrodialysis are accomplished with the help of semipermeable membrane in which liquid passes from the membrane and fluoride is retained upstream. The fundamental difference between membrane separation and electrodialysis is the driving force. Electrodialysis is performed under electrical field, while membrane separation is operated under pressure gradient. Although every technique has its benefits and drawbacks, selection of suitable method for fluoride removal is crucial and depends on various factors like cost, operating conditions, acceptance and further processing. For example, it was observed that bone char showed significant efficiency at low cost, but it may not be accepted by various communities; similarly, RO systems can remove upto 95% fluoride, but high cost and greater fluoride concentration in reject stream is major drawback for deprived population and places where water availability is low [5, 6]. So, it must be examined not only the water but also the surroundings for successful implementation of defluoridation for the selected place and population. Based on previous studies [7, 8], it was found that raw biomass and its derived adsorbents have good potential for the removal of fluoride owing to their availability, cost competence and overall performance.

Effects of the process parameters on fluoride removal can be studied by two different approaches, viz. single parameter conventional study and optimization with the help of different software. Several studies were performed through conventional single parameter study [9, 10]. Although conventional study provides initial idea of sorption process but does not tell about combine effect of operating parameters and cannot model the process. To solve this situation, process optimization can be performed by techniques such as genetic algorithm, artificial neural network (ANN), Taguchi and response surface methodology (RSM). The RSM and ANN are the most popular techniques for optimization and process modelling in fluoride removal [10–12] and similar operations [13, 14]. It is observed that most of the fluoride removal methods failed due to inefficient large-scale applicability and cost competence; still some applications have demonstrated community-based application [15, 16].

Dalbergia sissoo is recognized as Indian rosewood and used extensively in furniture industry for its termite resistance, strength and appearance. As expected, great quantity of sawdust is produced in the industry, which is waste, occupies space and causes health-safety issues. Thus, authors used this waste material to produce thermal activated *D. sissoo* sawdust (TADS) as potential adsorbent removes fluoride from potable water. The work is succession of the previous work [17] in which a suitable mechanism was developed to reduce fluoride in potable water. Here, the raw material was processed to prepare the adsorbent and conventional method was executed to assess effects of process parameters and operational range. Further, optimization, mathematical model development and prediction of removal were performed by response surface methodology (RSM) and artificial neural network (ANN). Some characterization techniques and parameter evaluation were also performed to support the study. It is worthy to mention that the literature could not be found on the application of TADS for such study which provides the novelty to the present study.

Experimental Section

Sorption Experiment

A 100 mg/L of standard fluoride solution was prepared by dissolving NaF (CDH, India) in double-distilled deionized water and suitably diluted. The pH of solution was measured by pH metre (Hanna Instruments Inc.) and altered by adding HCl or NaOH (CDH, India). The waste *D. sissoo* sawdust of nearby furniture shop was initially cleaned by normal water to eliminate water-soluble contaminants and dirt and subsequently rinsed by distilled water. The sawdust was then dried for 6 h at 80 °C in hot air oven (Satyam Sci. Ins. Ind., India). The sawdust was filled in airtight stainless steel cylinder, tapped to remove any void space and subjected to 800 °C to prepare the thermal activated *D. sissoo* sawdust (TADS) [18]. The charred material was screened to

J. Inst. Eng. India Ser. E (December 2022) 103(2):323–337

325

obtain 100–125 µm particles, which were the largest fraction and popular among researchers [19, 20]. Subsequently, the sieved TADS was kept in airtight vessel for experimental use. Some properties of prepared TADS are determined [21, 22] and mentioned in Table 1.

The batch study was executed in two phases; first to examine dependency of fluoride sorption on operating parameters by convention single parameter study, secondly the optimization by RSM and ANN. The process parameters were ranged as per the previous studies [23] as pH (2–12); fluoride concentrations (0–15 mg/L); TADS dose (0–20 g/L); time (0–3 h) and temperature (15–45 °C). Experiments were performed in incubator-shaker (Chino Sci. Inst. Mfg, India) at constant swirling at 150 rpm in a 250 mL flask. Samples were withdrawn after the experiment, filtered, suitably diluted, and resulting fluoride concentration was evaluated by the SPADNS method [24]. Observations were taken in triplets, and mean value was used to calculate removal as depicted in Eq. (1).

% Removal

$$= \frac{\text{Initial conc. of fluoride} - \text{Final conc. of fluoride}}{\text{Initial conc. of fluoride}} \times 100 \quad (1)$$

Results obtained from batch study were utilized to extend the understanding of sorption process. The concentration dependency was applied to investigate the sorption isotherms, while contact time-related data were used in kinetics. Similarly, temperature-associated fluoride removal helped in the thermodynamic investigations. A flow chart consisting various steps of experiments is presented in Fig. 1.
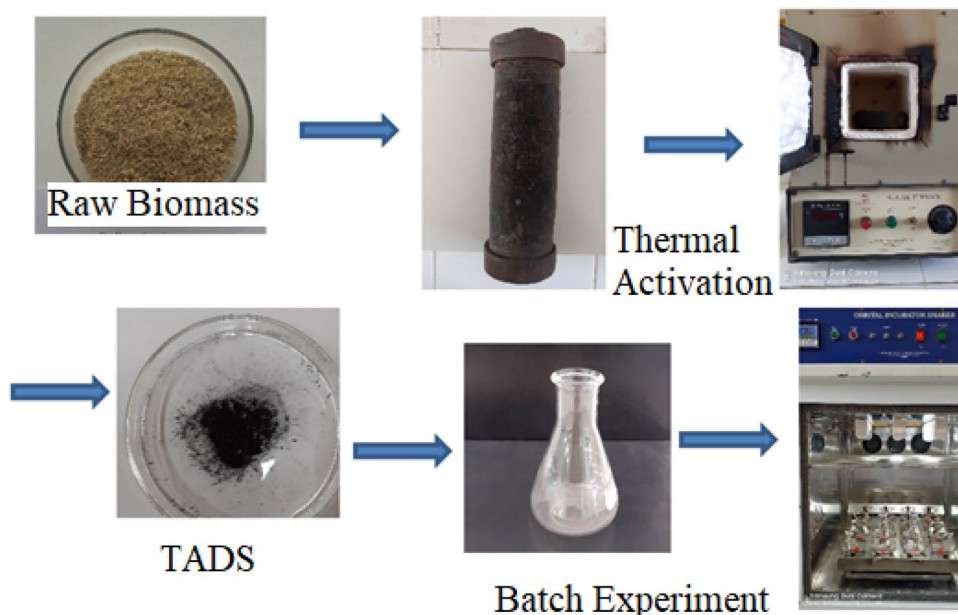
SEM- EDS, Zeta Potential and FTIR Analyses

Surface morphology of TADS prior and posterior to the fluoride adsorption was investigated with SEM–EDS (Tescan, MIRA3). The sample was applied on carbon-coated copper grid and sputtered with Pd plasma coating. The sample was finally placed in the chamber to produce images. SEM image of TADS after the fluoride sorption reflected some morphological changes in TADS and thus indicated fluoride attachment onto the adsorbent. The new peak of fluoride in EDS spectrum confirmed the attachment of fluoride on TADS after the sorption. The participation of functional groups in adsorption was identified by FTIR (Bruker, Alpha T) analysis. FTIR was performed by subjecting the adsorbent to moderate heat for initial drying at room temperature followed by pellet formation. The prepared pallet was then placed in the instrument to record the FTIR spectra. Moreover, zeta potential at various solution pH of TADS suspension was evaluated by a zeta potential analyzer (Malvern,

Table 1 TADS characteristic

Parameter	Value
Loss in ignition	77.8
Area (m²/g)	242
Density (kg/m³)	520
pH	6.1
Moisture (%)	4.3
Volatile components (%)	14.2
Ash (%)	11.1
Fixed carbon (%)	70.4

Fig. 1 Flow chart showing various steps performed in the study

Raw Biomass

Thermal Activation

TADS

Batch Experiment

326

J. Inst. Eng. India Ser. E (December 2022) 103(2):323–337

Zeta Sizer Nano ZS90) to check point of zero charge, i.e. pH_{ZpC}. The adsorbent was firstly dissolved in deionized water, and the pH of prepared suspensions was adjusted between 2 and 12 with the help of 0.01 N NaOH or 0.01 N HCl. The well-mixed suspension was then subjected to zeta potential analyzer to produce the reading.

Optimization by RSM

Although the conventional single parameter study gives us the initial idea of sorption process and talks about the effect of operating parameters; it lacks at various aspects as it does not mansion about combine effect of operating parameters, relative potency of these operating parameters, and most importantly, it cannot mathematically modeled the sorption process; thus, it is not possible to predict the adsorption at some random set of operating parameters. To address these problem optimizations of process is necessary which can be performed with help of various software. RSM is one of the promising optimization methods for process optimization. The 3-level 4-factor RSM-based Box–Behnken design (BBD) was used in the present study to examine sorption process. BBD is a spherical, revolving RSM design having a central point, mid points of edges of cube confined on the sphere [25]. A generalized equation to represent relation among dependent (Y), independent variable (x) and error (ε) can be written and presented in Eq. 2.

$$Y = f\left(X_i, X_j \ldots X_n\right) + \varepsilon \tag{2}$$

The pH, TADS dose, fluoride concentration and time were chosen as independent variable, whereas removal was the dependent variable in the study. As the temperature did not affect the process critically, it was kept constant at 25 °C. Equation (2) is more generic representation which is elaborated in result section for model-specific discussion. Levels of parameters for low, central point and high were coded as −1, 0 and 1 as given in Table 2. Equation (3) is applied to calculate the number of experiments for 4 factors (represented as "k") and 5 central points (represented as "C_0").

Table 2 Process parameter and respective BBD levels

Process variables	Level		
	− 1 (Low)	0 (Centre point)	1 (High)
Solution pH (X_1)	2	7	12
Fluoride Concentration (mg/L) (X_2)	5	15	25
CADS Dose (g/L) (X_3)	2	11	20
Contact Time (min) (X_4)	10	95	180

$$\text{Number of run} = 2k(k - 1) + C_0 \tag{3}$$

Twenty-nine experiments depicted in Table 3 were recommended by Design Expert (Trail Version11, Statease Inc., USA) and performed accordingly. Various mathematical models were tested with the experimental observations to acquire the model. The competence of models was tested by sequential model sum of squares and model summary by applying coefficient of determination (R^2) and similar parameters [26]. Once the model was selected, equation was developed to express removal in terms of process parameters. The model and significance of process parameters were evaluated by ANOVA by P and F values. In the next step, three-dimensional graphs were produced to observe combined effects of operating parameters, and optimized process conditions were explored.

Construction of ANN Model

Artificial neural network (ANN) is very beneficial for simulation and process optimization. It is a mathematical model that works like the biological neural network, learns by iteration and does not need prior information of parameters, thus solving complex computing by following pattern of similar previous problems. ANN performs parallel computing for data processing, learns by patterns, does not follow any specific rules, or learns through a specified system unlike traditional methods. ANN evaluates results for provided inputs, compares the results with provided-outputs and rectifies the deviations. The rectification continues till the calculated results, and provided-outputs have least variation. The ANN has input, hidden and output layer for observations, processing and results, respectively. The input observations (nodes) are connected with hidden layer with interconnection and weight updation. The hidden layer is further connected with output through bias and activation function. While the weight and bias adjust the inputs, activation function converts linear input into non-linear to learn and perform computation [27, 28]. A simplified relation among various entities of ANN can be written in Eq. (4) as

$$\text{Output} = f_{\text{activation}}\{(\text{Input} * \text{Weight}) + \text{Bias}\} \tag{4}$$

The MATLAB (R2013a Mathworks, Inc)-based NFTOOL was employed to generate ANN model. The ANN model was constructed from 53 dataset obtained from conventional and BBD model and divided into three segments as training (37 samples, i.e. 70%), testing (8 samples, i.e. 15%) and validation (8 samples, i.e. 15%). A three-layer feedforward BP model was selected consisting of 5 inputs, viz. pH, dose, fluoride concentration, contact time and temperature; 10 neurons in hidden layer and 1 output neuron as % of fluoride removal. The temperature parameter was not

J. Inst. Eng. India Ser. E (December 2022) 103(2):323–337

327

Table 3 Run order, operating parameter, actual and predicted removal

Run order	Solution pH (Coded value)	TADS Dose (Coded value) (g/L)	F Conc. (Coded value) (mg/L)	Time (Coded value) (min)	Actual Removal	RSM Predicted Removal	ANN Predicted Removal
1	12 (+1)	15 (0)	2 (−1)	95 (0)	65.00	63.81	56.0248
2	12 (+1)	15 (0)	20 (+1)	95 (0)	20.00	23.98	29.7103
3	7 (0)	25 (+1)	11 (0)	10 (−1)	20.00	25.56	29.9672
4	7 (0)	15 (0)	11 (0)	95 (0)	32.70	32.70	45.0911
5	2 (−1)	15 (0)	20 (+1)	95 (0)	48.50	55.41	34.2253
6	7 (0)	15 (0)	11 (0)	95 (0)	32.70	32.70	20.0058
7	7(0)	5 (−1)	20 (+1)	95 (0)	32.50	27.74	32.3871
8	7 (0)	15 (0)	11 (0)	95 (0)	32.70	32.70	32.2284
9	2 (−1)	15 (0)	11 (0)	10 (−1)	28.20	30.62	32.3871
10	12 (+1)	25 (+1)	11 (0)	95 (0)	56.40	45.57	31.9652
11	2 (−1)	15 (0)	2 (−1)	95 (0)	75.00	76.74	66.6222
12	7 (0)	15 (0)	11 (0)	95 (0)	32.70	32.70	28.1675
13	7 (0)	25 (+1)	20 (+1)	95 (0)	43.00	42.82	55.9141
14	7 (0)	15 (0)	2 (−1)	10 (−1)	50.00	42.72	42.2284
15	12 (+1)	15 (0)	11 (0)	180 (+1)	24.50	23.97	33.0079
16	7 (0)	25 (+1)	11 (0)	180 (+1)	30.00	37.89	42.8483
17	7 (0)	5 (−1)	2 (−1)	95 (0)	55.00	57.07	50.046
18	7 (0)	15 (0)	20 (+1)	10 (−1)	22.50	16.89	30.1336
19	12 (+1)	5 (−1)	11 (0)	95 (0)	12.70	14.19	15.6255
20	7 (0)	5 (−1)	11 (0)	180 (+1)	24.60	24.76	34.8533
21	2 (−1)	5 (−1)	11 (0)	95 (0)	48.20	51.42	42.21
22	12 (+1)	15 (0)	11 (0)	10 (−1)	2.70	9.79	6.425
23	2 (−1)	25 (+1)	11 (0)	95 (0)	61.80	52.70	60.9525
24	7 (0)	15 (0)	20 (+1)	180 (+1)	28.00	27.67	12.931
25	2 (−1)	15 (0)	11 (0)	180 (+1)	52.70	47.50	63.6153
26	7 (0)	15 (0)	2 (−1)	180 (+1)	65.00	63.00	61.6057
27	7 (0)	5 (−1)	11 (0)	10 (−1)	8.20	6.03	7.7901
28	7 (0)	25 (+1)	2 (−1)	95 (0)	68.00	74.65	65.0958
29	7 (0)	15 (0)	11 (0)	95 (0)	32.70	32.70	23.9556

included in RSM as it is impractical to increase temperature of large quantity of potable water and again decrease it to room temperature in community-based applications. So, to avoid delusion, the temperature was kept constant at 25 °C in RSM-based optimization. Yet, it was considered as an operating parameter (constant at 25 °C) while constructing ANN model. The addition of temperature in ANN model would increase number of nodes and ultimately the accuracy in the prediction of removal.

Result

Single Parameter Study

The single parameter, i.e. conventional study was conducted to understand the impact of individual parameter on

fluoride adsorption and to find appropriate operating range. The study was performed by suitably increasing the process parameter in prescribed range, while remaining parameters were not altered. Thus, effects of operating parameters were studied and presented in Fig. 2. Fluoride removal was inversely affected by solution pH (Fig. 2a) and fluoride concentration (Fig. 2b), on the other hand, increases in TADS dose (Fig. 2c) and time (Fig. 2d) showed higher removal.

The sorption sites present on TADS surface got protonation of in acidic medium, and thus, higher sorption of fluoride species in acidic region was achieved. Further, adsorption decreased in alkaline medium solution pH due to decreased protonation and increased OH^- in solution. The zeta potential (pH_{zpc}) analysis was further performed (Fig. 2e) to determine the surface charge distribution. It is the solution pH where net charges on adsorbent are neutral. Adsorbent will attract cationic species at pH higher
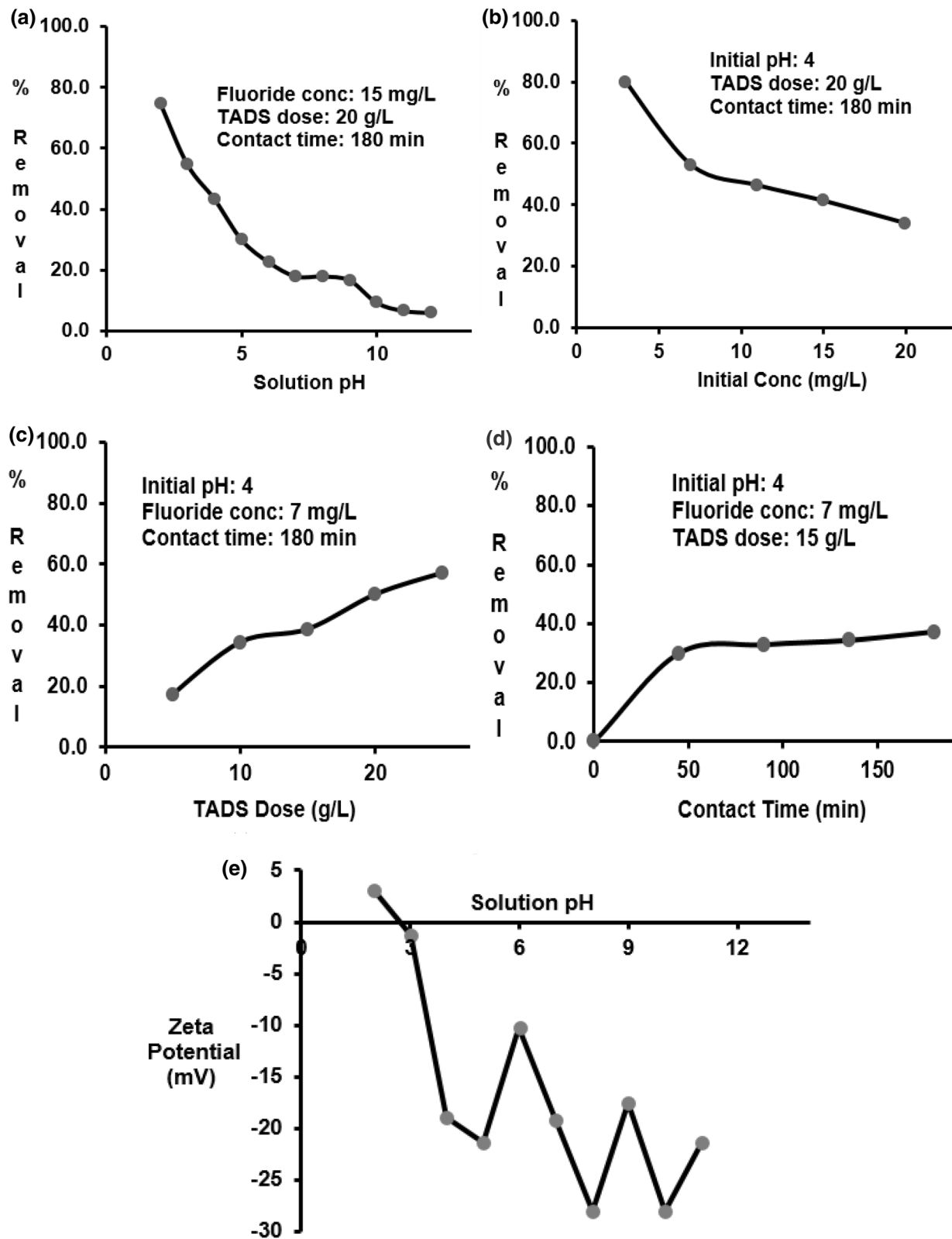
Fig. 2 Effect of operating parameters (**a–d**) on fluoride sorption, zeta potential of TADS (**e**)

than pH_{zpc}, while anions at pH less than pH_{zpc} [29]. It was seen that the curve changed its polarity about pH 3, and by interpolation, the pH_{zpc} value was determined to be 2.9. The result was in close resemblance to the effect of solution pH. Dependency of fluoride removal on fluoride concentration is evaluated and shown in Fig. 2b where removal decreased from 80 to 40% as the fluoride concentration increased from 3 to 20 mg/L. Continuous reduction in the removal percentage was as a result of increased competition among fluoride ions to get attached to the sorption sites. Result represented in Fig. 2c displayed effect of adsorbent dose on fluoride removal. The removal of fluoride increased as the adsorbent dose increased due to the enhanced number of adsorption sites. Almost analogous results are obtained in Fig. 2d where dependency of fluoride removal on contact time was evaluated. Continuous increase (upto 40% removal) in 60 min was observed at initial, but the removal was virtually constant after 60 min which is attributed by the slow diffusion of fluoride on TADS adsorption sites. The higher fluoride removal at higher value of TADS dose and contact time was natural effect of increased availability of sorption sites and time although they were insignificant at very high values [30].

## Thermodynamics and Kinetics of Fluoride Sorption

Study to observe effect of temperature on sorption gave us opportunity to understand thermodynamic. The study presented in Fig. 3a, b showed dependency of sorption on temperature and relation between temperature and distribution coefficient (K_D). Further, relation among change in enthalpy (ΔH), change in Gibbs free energy (ΔG) and change in entropy (ΔS) was established by applying basic parameters, viz. initial concentration (C_0), equilibrium concentration (C_e), volume (V), mass of adsorbent (m), gas constant (R) and temperature (T) are presented in Eq. (5–7) as suggested by previous studies [31].

$$K_D = \frac{(C_0 - C_e)V}{C_e * m} \tag{5}$$

$$\ln K_D = \frac{\Delta S}{R} - \frac{\Delta H}{RT} \tag{6}$$

$$\Delta G = \Delta H - T\Delta S \tag{7}$$

Fig. 3 Effect of temperature (**a**), relation with K_D (**b**), kinetics of fluoride sorption on TADS (**c**)

330

J. Inst. Eng. India Ser. E (December 2022) 103(2):323–337
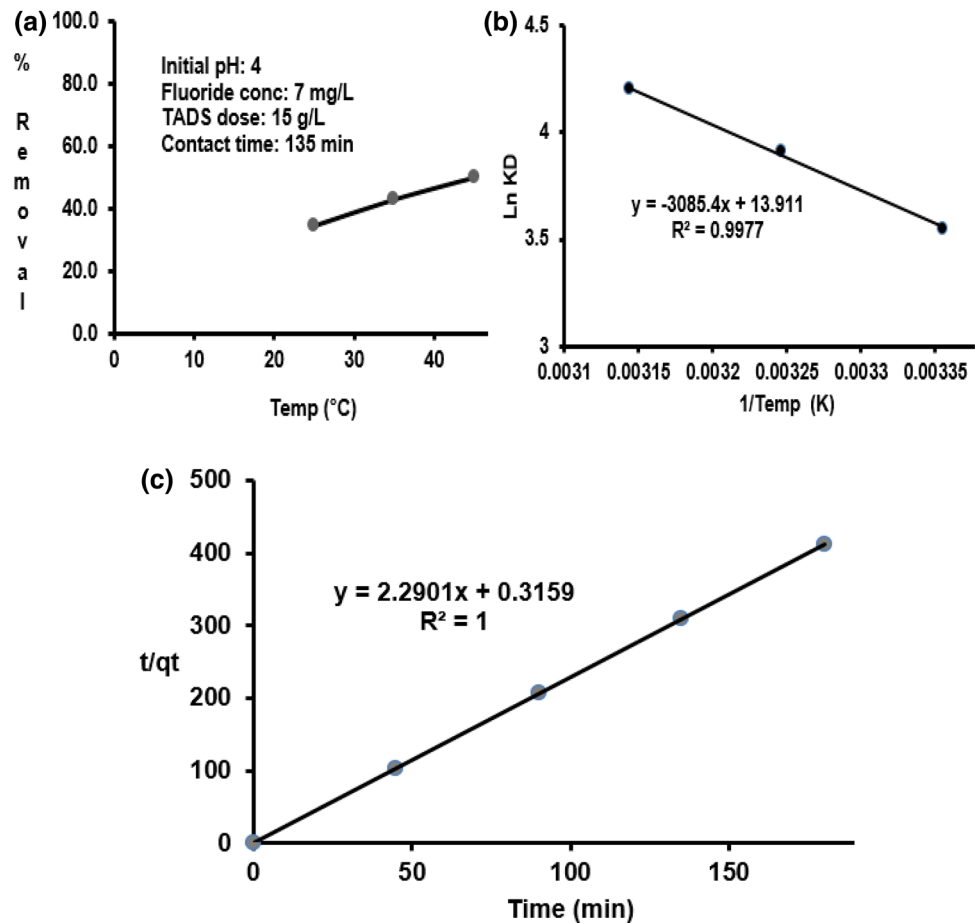
The ΔG evaluated within -8813.5 to $-11{,}126.6$ kJ/mol, while ΔS and ΔH were calculated to be 115.6 kJ/mol and 25,652 kJ/mol K, respectively. Results obtained from Fig. 3b, and respective calculation supports the sorption phenomenon and gave the further clarity. Spontaneous and endothermic nature of sorption was confirmed by negative ΔG. Similarly, positive ΔH further confirmed endothermic nature of process. The positive ΔS showed affinity of TADS towards fluoride, and results are in close resemblance with earlier works [32].

Fluoride sorption on TADS was explained by pseudo-second-order kinetics. The model implied that fluoride removal was governed by chemisorption and the rate was fluoride and TADS dependent. The model was examined by R^2 by plotting concentration data against time. Mathematical expressions to relate fluoride adsorbed (q_t), time (t), adsorption capacity (q_{max}) and rate constant (k_2) are presented in Eq. 8 [33].

$$\frac{1}{q_t} = \frac{1}{k_2 q_{max}^2} + \frac{t}{q_{max}} \tag{8}$$

When t/q_t was plotted against t (Fig. 3c), the slope gave equilibrium sorption capacity and intercept gave rate constant. The rate constant and the adsorption capacity were calculated as 14.96 g/mg*min, 0.5 mg/g, respectively, while the R^2 was unity.

Isotherm Study

Adsorption isotherms models were analysed to understand the type of adsorption and fluoride distribution on TADS surface in solid–liquid system. Two most popular isotherms (Langmuir, Freundlich) were studied at constant solution pH 4, TADS dose 15 g/L, 135 min and 25 °C temperature. Although solution pH 4 is acidic in nature yet it was selected as benchmark for experiments and similar trend can be expected for neutral range for optimization purpose. Fluoride was gradually increased from 0 to 20 mg/L in the study. Langmuir isotherm suggested monolayer adsorption on homogeneous surface. Its linear form (Eq. 9) was plotted to calculate monolayer adsorption capacity. Fluoride adsorbed was represented as q_e (mg/g), q_{max} (mg/g) as monolayer adsorption capacity, while b was the constant (L/mg) showing affinity of binding sites. Further, Freundlich model explained multilayer sorption on heterogeneous surface. The Freundlich model written in Eq. 10 where K_F is related to relative adsorption capacity (mg/g), $1/n$ indicates intensity of sorption [34].

$$\frac{C_e}{q_e} = \frac{1}{q_{max}b} + \frac{C_e}{q_{max}} \tag{9}$$

$$\ln q_e = ln k_F + \frac{1}{n} ln C_e \tag{10}$$

The q_{max} and b for Langmuir isotherm were calculated as 0.7 mg/g and 0.2 L/mg. The calculated values of K_F and $1/n$ were 0.5 mg/g and 0.2 Freundlich model confirmed that adsorption was favourable.

SEM- EDS and FTIR Analyses

Morphology of adsorbent prior and posterior of sorption was examined by SEM–EDS as presented in Fig. 4. Figure 4a shows that surface of adsorbent is highly porous and rough before the sorption, which can be considered as an indication of virgin adsorbent. On the other hand, some brighter spots on the TADS surface in Fig. 4b can be seen as fluoride salts deposited after fluoride adsorption. These brighter spots could be the result of burnt material, so the evidence of fluoride adsorption was further examined by EDS. The EDS images of TADS before
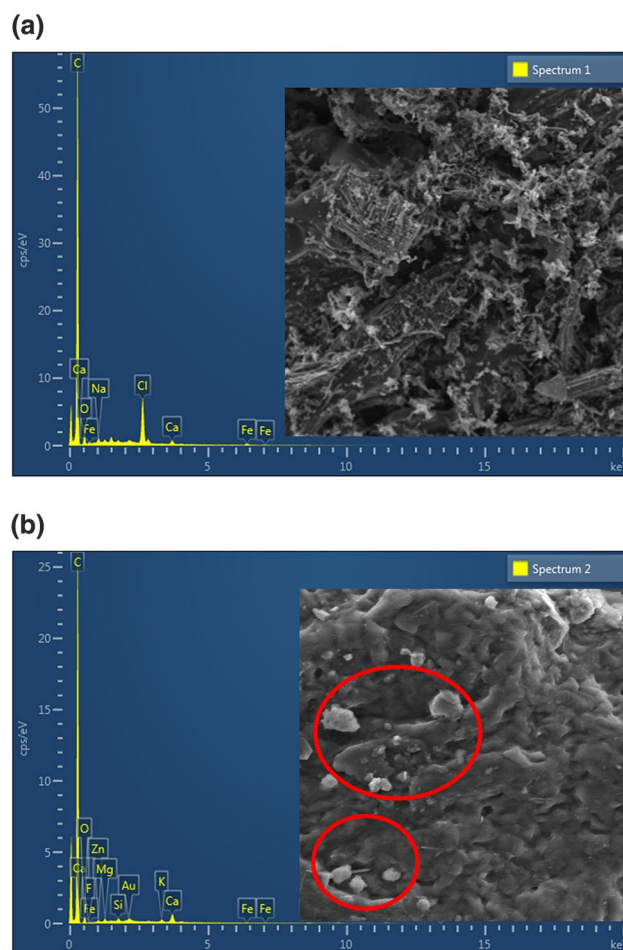

(a)

(b)

Fig. 4 SEM and EDS of TADS before (**a**) and after (**b**) fluoride sorption

and after fluoride sorption are also presented in the same figures. The new peaks of fluoride emerged in Fig. 3 are an evidence of fluoride attachment to TADS which was absent before the sorption.

The FTIR conducted prior and post-sorption provided insight of fluoride removal mechanism. The FTIR spectrum gave the peaks for respective functional groups attached to the surface of adsorbent. Thus, if a specific group is associated with sorption; it will either be modified or may disappear. Spectrum of virgin and exhausted TADS was recorded in 4000–600 cm^{-1} region at 2 cm^{-1} resolution (Fig. 5). Figure shows peaks in 3800–3500 cm^{-1} range for O–H and N–H group, 3300–2500 cm^{-1} for primary and secondary amines, OH^-, $COOH^-$, while 2357 cm^{-1} peak indicated O=C=O stretch. Further, C=O stretching was displayed by 1750 to 1650 cm^{-1} peaks and 1550 to 1500 cm^{-1} indicated nitro compound. By the examination of FTIR spectra after the fluoride adsorption, it was found that these peaks were vanished or reduced or shifted. These alterations in spectrum peak exhibited the involvement of these functional groups in fluoride sorption. Some new peaks were found in 1400 to 550 cm^{-1} band after adsorption stating the appearance of the fluoro compound [35, 36].

Optimization by RSM

The second order, i.e. quadratic model was selected for further investigation. This model was selected because its P value was less than 0.0001, variance inflation factor was 1.0, standard deviation was 6.6, Adeq Precision was14.7 and R^2 was 0.94. Although cubical model showed highest values of R^2, etc., among all models suggested (Table 4), it was found to be aliased and rejected due to repeated entities. This model can be derived to correlate removal (dependent variable, Y), process parameters (independent variable, x), number of variables (n), interactive coefficients (b) and error (ε) as described in Eq. (11).

$$Y = b_0 + \sum_{i=1}^{n} b_i x_i + \sum_{i=1}^{n} b_{ii} x_i^2 + \sum_{i<j}^{n} \sum_{j}^{n} b_{ij} x_i x_j + \varepsilon \qquad (11)$$

This empirical relationship was fitted to observations based on BBD model and respective inputs. The equation to relate fluoride removal with process parameters in actual terms is written in Eq. (12). Results are also represented in Fig. 6a for better representation where points near to the line showed closeness of actual and predicted value and vice-versa.

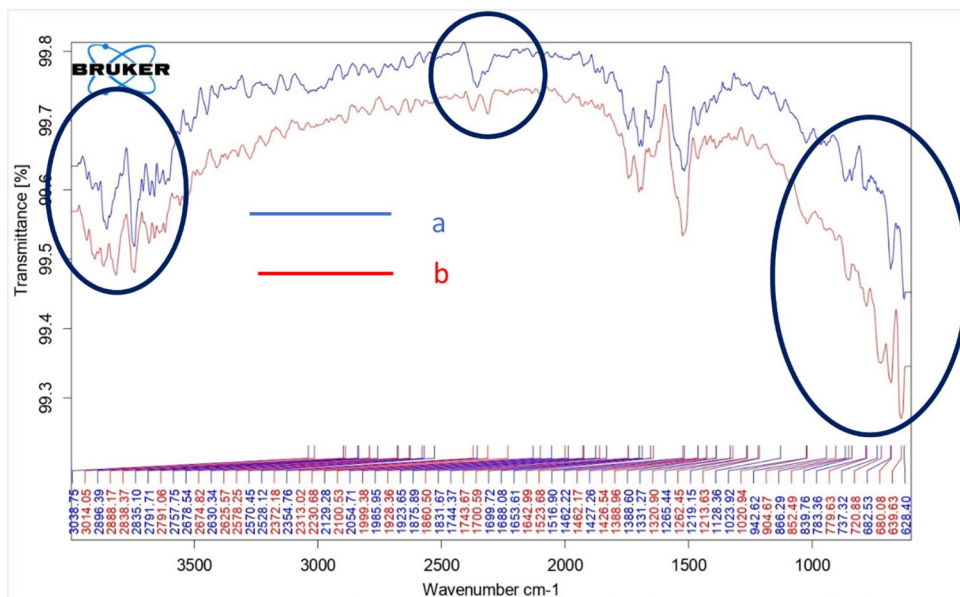**Fig. 5** FTIR of TADS before (**a**) and after (**b**) fluoride sorption

Table 4 Model fit summery for fluoride by TADS

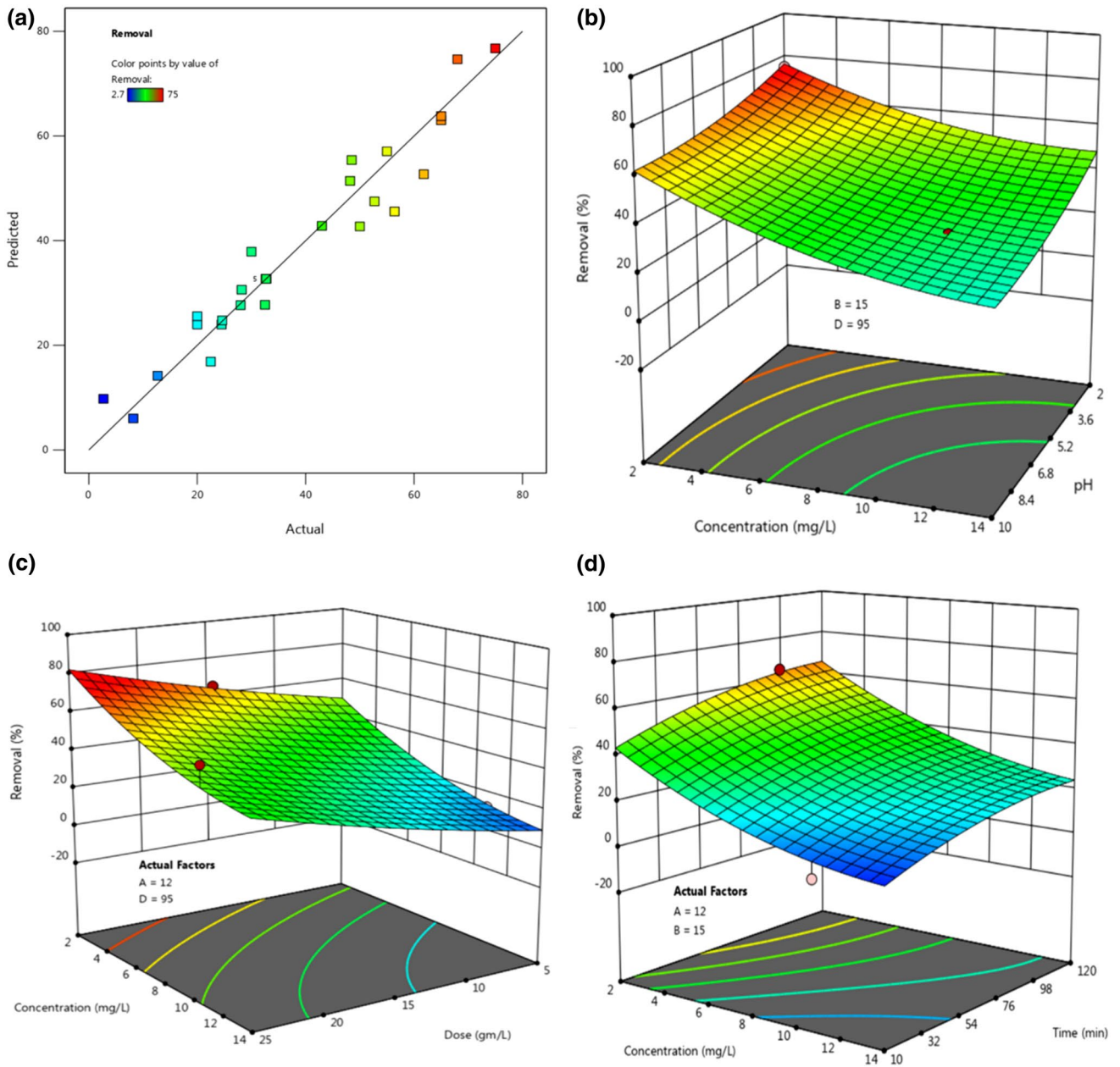| Source	SD	R^2	Adjusted R^2	Predicted R^2	Press	
Linear	13.18	0.5821	0.5125	0.3525	6458.70	
2FI	14.57	0.6170	0.4043	−0.2380	12,349.11	
Quadratic	6.66	0.9377	0.8753	0.6410	3581.15	Suggested
Cubic	5.60	0.9811	0.9119	−1.7182	27,113.88	Aliased

Fig. 6 Actual and predicted fluoride removal (**a**), Interactive effect of operating parameter (**b–d**). Operating parameter: A = pH, B = adsorbent dose, C = fluoride conc., D = time

$$Removal = +72.50314 - 6.74573\,pH + 0.560371\,\text{Dose} - 4.91036\,\text{Concentration} + 0.456012\,\text{Time} + 0.150500\,(pH * \text{Dose}) - 0.102778\,(pH * \text{Concentration})$$
$$- 0.001588\,(pH * \text{Time}) - 0.006944\,(\text{Dose} * \text{Concentration}) + 0.001882\,(\text{Dose} * \text{Time}) - 0.003105\,(\text{Concentration} * \text{Time}) + 0.253667\,pH^2 \qquad (12)$$
$$+ 0.019292\,\text{Dose}^2 + 0.196811\,\text{Concentration}^2 + 0.001532\,\text{Time}^2$$

Table 5 ANOVA for fluoride removal by TADS

Source	Sum of squares	df	Mean square	F-value	p value
Model	9353.12	14	668.08	15.04	<0.0001
A-pH	1476.30	1	1476.30	33.24	<0.0001
B-Dose	800.33	1	800.33	18.02	0.0008
C-Concentration	2806.02	1	2806.02	63.19	<0.0001
D-Time	723.85	1	723.85	16.30	0.0012
AB	226.50	1	226.50	5.10	0.0404
AC	85.56	1	85.56	1.93	0.1868
AD	1.82	1	1.82	0.0410	0.8424
BC	1.56	1	1.56	0.0352	0.8539
BD	10.24	1	10.24	0.2306	0.6385
CD	22.56	1	22.56	0.5081	0.4877
A^2	260.87	1	260.87	5.87	0.0295
B^2	24.14	1	24.14	0.5436	0.4731
C^2	1648.45	1	1648.45	37.12	<0.0001
D^2	795.01	1	795.01	17.90	0.0008
Residual	621.73	14	44.41		
Lack of Fit	621.73	10	62.17		
Pure Error	0.0000	4	0.0000		
Cor total	9974.85	28			

These model terms were examined by ANOVA to evaluate their relative potency to affect the process as represented in Table 5. The model was significant as sum of square was 9353.12, F value was 15.04 and P value was < 0.0001. Some significant term that affected the sorption process was pH, Dose, Concentration, Time, pH*Dose, pH^2, $Dose^2$, $Concentration^2$ and $Time^2$ as their P values were less than 0.05 and higher F value.

The 3-D surface plots construction was an important aspect of RSM study. This helped to observe interactive effect of parameter on the fluoride removal. The three-dimensional plots were created by changing two parameters in given range, while others were kept at fixed levels. Figure 6b–d represents combination of operating parameters and fluoride removal for given conditions at 25 °C temperature.

Figure 6b shows effect of solution pH (2–10) and fluoride concentration (2–14 mg/L) at 15 g/L TADS dose and 95 min contact time. It could be seen that fluoride removal was as low as 0% and high as 80% in the operating range. It is also clear that as the pH and concentration increased removal decreased which is again in close resemblance with single parameter study. In the same way, concentration–dose effect is presented in Fig. 6c. The fluoride concentration varied in 2–14 mg/L range; TADS dose varied between 5 and 25 g/L, while pH and time were 12 and 95 min. For above-said conditions, fluoride removal was

expected between 0 and 80%. The 6(d) plot represents relation among fluoride concentration (2–14 mg/L), contact time (10–120 min) and fluoride removal at 12 pH and 15 g/L TADS dose. The fluoride removal likely to fall in the range of 0 to 65% by following the same trend as depicted in conventional methodology.

As the three-dimensional plot depicts the expected removal for given set of conditions, next phase of the study was to find optimized conditions for a substantial fluoride removal. These conditions were developed by the software utilizing the mathematical model. The solution pH 6.0, TADS dose 12.0 g/L, 8.0 mg/L fluoride, 90 min contact time and 25 °C temperature were selected for prediction. Expected removal was mentioned as 33% to 45% with about 6% standard deviation. Further, the optimization was validated by conducting the experiments for above-said conditions. The removal was found to be 42% which was very close to the expected value and thus validated the model.

ANN Model Construction and Validation

The proposed ANN model would not simply perform without a suitable algorithm and activation function. The model was trained by applying Levenberg–Marquardt back propagation (LM-BP) algorithm. The hidden layer was associated with hyperbolic sigmoid transfer function (TANSIG), while PURELIN function was linked with output layer. The observations were divided into 3 sets, viz. 37 (70%) for training, 8 (15%) for testing and 8 (15%) for validation. Training was performed to adjust the ANN according to the error; validation was used to measure network generalization, while testing was an independent measure of network performance. The network was retrained several times to get highest regression values (R) and lowest mean square error (MSE) for testing, validation and training [37]. The TANSIG, PURELIN and MSE functions for "n" variables can be expressed in Eq. (13–15).

$$tansig(n) = \frac{2}{1 + \exp(-2n)} - 1 \tag{13}$$

$$purelin(n) = n \tag{14}$$

$$MSE = \frac{1}{n} \sum_{1}^{n} (actual\ value - predicted\ value)^2 \tag{15}$$

The generalized architecture of proposed ANN model is depicted in Fig. 7a. At 16th iteration, the R-value for training, validation and test was calculated as 0.97, 0.92 0.88 and MSE as 24, 42 and 99 presented in Fig. 7b. The constructed model was saved, and fluoride removal at any given condition could be predicted by it.

Fig. 7 ANN model: architecture (**a**), *R*-value for training, validation, test and overall performance (**b**)
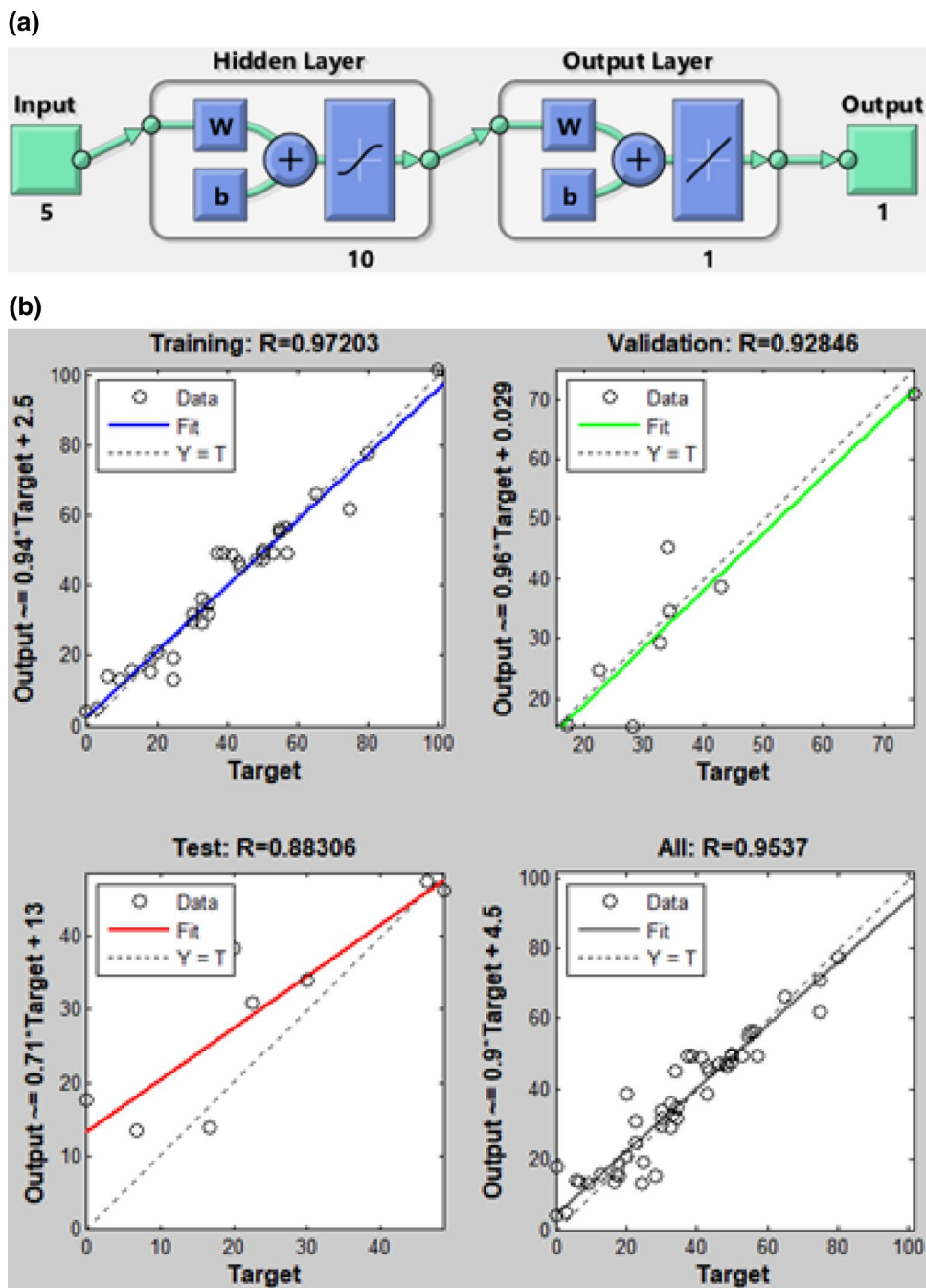
Accuracy of the ANN model was confirmed by predicting the fluoride removal at pH 6.0, TADS dose 12.0 g/L, 8.0 mg/L fluoride, 90 min contact time and 25 °C temperature. At the selected operating conditions, the model predicted 37% removal, while actual removal was calculated as 42% at the same operation conditions. Although a marginal difference of 5% is observed, still, the model can be considered as a successful attempt for the prediction of fluoride removal. The ANN predicted removal was further compared with RSM predicted removal. The above-stated process condition, i.e. pH 6.0, TADS dose 12.0 g/L, 8.0 mg/L fluoride, 90 min contact time and 25 °C temperature was fed into The RSM model. For these given conditions, RSM predicted 45% fluoride removal which is again close to the actual removal (42%). From the comparison of both models, it can be concluded that RSM prediction was slightly better than the ANN model.
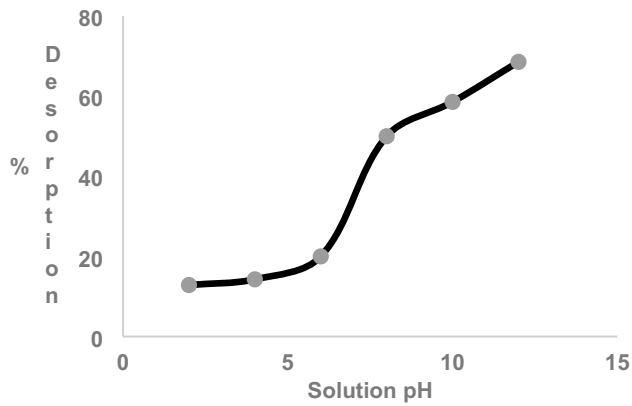
Fig. 8 Effect of solution pH on desorption of fluoride

Table 6 Field study of TADS

S. no	Parameter	Concentration before	Concentration after
1	pH	7.9	7.6
2	Total dissolved solids (mg/L)	1220	1150
3	Fluoride (mg/L)	4.2	1.2

Regeneration of Adsorbent

Once the adsorbent surface is saturated, it would not adsorb adsorbate present in solution. So, new adsorbent is required to perform the sorption, while disposal of saturated adsorbent causes environmental load and increased overall cost. Both problems can be overcome by regenerating the saturated adsorbent. Desorption of fluoride was studied in pH range 2–12 with HCl or NaOH. Desorption was performed using 0.37 g fluoride loaded TADS in 100 mL distilled water with different pH for 135 min 150 rpm agitation. The operating conditions were similar to the conventional study described earlier, and fluoride concentration was measured in solution. Effect solution pH on fluoride desorption presented in Fig. 8 showed that desorption was very low in acidic pH, indicating the possible desorption of saturated TADS in basic medium [38]. It was found that 58% desorption was achieved at pH 10, while more than 65% fluoride was desorbed at pH 12. Higher desorption in basic medium was due to leaching of bound fluoride ions from TADS surface. Therefore, fluoride loaded TADS can be regenerated using NaOH solution indicating the reusability of TADS. Still, further investigation is expected to determine life cycle of the regenerated TADS.

Field Study

Fluoride removal efficiency of TADS bioadsorbent was finally checked for water sample collected nearby. The sample was subjected to few water quality assessment tests, and results for the respective parameters are shown in Table 6. A 1.0 g of TADS was added in 100 mL water sample and kept in contact for 60 min 25 °C temperature. Table 6 also presents the results of analysis after the sorption process. The result of TADS adsorbent was quite optimistic as it reduced fluoride concentration well below the acceptable limit, and other parameters of water were also improved. So, the TADS adsorbent is found to be useful for aqueous-based fluoride removal.

Conclusion

The presented work showed that TADS is a useful adsorbent to remove fluoride from water. Maximum adsorptive removal was achieved around 80% at pH 2, fluoride concentration 15 mg/L, TADS dose 20 mg/L, contact time 180 min and temperature 25 °C. The fluoride removal enhanced with increase in TADS dose, time and temperature, while pH and fluoride concentration showed negative effect. Data of concentration used in Langmuir and Freundlich isotherms explained adsorption process and sorption capacity were calculated as 0.7 mg fluoride/g TADS. Study of thermodynamic entities ΔH, ΔS, ΔG revealed spontaneous and endothermic nature of fluoride sorption. Zeta potential analysis showed charge neutralization occurred at 2.9 pH, and SEM–EDS confirmed morphological changes in TADS during the sorption. RSM-BBD and ANN model were generated, and optimized conditions for fluoride removal were predicted. Lastly, regeneration in basic medium was performed to establish the use of *D. sissoo* modified adsorbent for fluoride removal as an environmentally friendly and economic process. It is quite possible that reader may find other adsorbents which may exhibit higher removal efficiency, yet application of waste, abundant quantity and free of cost sawdust provides a notch over other materials which have may not be available with others.

Declarations

Conflict of interest No conflict of interest.

336

J. Inst. Eng. India Ser. E (December 2022) 103(2):323–337

References

1. S. Zhang, Y. Lu, X. Lin, X. Su, Y. Zhang, Removal of fluoride from groundwater by adsorption onto La (III)–Al (III) loaded scoria adsorbent. Appl. Surf. Sci. **303**, 1–5 (2014)

2. M.K. Shahid, J.Y. Kim, G. Shin, Y. Choi, Effect of pyrolysis conditions on characteristics and fluoride adsorptive performance of bone char derived from bone residue. J. Water Process Eng. **37**, 101499 (2020)

3. S. Dey, B. Giri, Fluoride fact on human health and health problems: a review. Med. Clin. Rev. **2**(1), 11 (2016)

4. Bureau of Indian Standards. Draft Indian standard-drinking water specification Second Revision of IS 10500. New Delhi; 2009.

5. S.V. Jadhav, E. Bringas, G.D. Yadav, V.K. Rathod, I. Ortiz, K.V. Marathe, Arsenic and fluoride contaminated groundwaters: a review of current technologies for contaminants removal. J. Environ. Manage. **162**, 306–325 (2015)

6. Z. Hussain, L. Daosheng, L. Xi, K. Jianxiong, Defluoridation by a Mg–Al–La triple-metal hydrous oxide: synthesis, sorption, characterization and emphasis on the neutral pH of treated water. RSC Adv. **5**(55), 43906–43916 (2015)

7. S. Ghosh, A. Malloum, C.A. Igwegbe, J.O. Ighalo, S. Ahmadi, M.H. Dehghani, A. Othmani, Ö. Gökkus, N.M. Mubarak, New generation adsorbents for the removal of fluoride from water and wastewater: a review. J. Mol. Liq. **346**, 118257 (2022)

8. S. Rangabhashiyam, P.V. dos Santos Lins, L.M. de Magalhães Oliveira, P. Sepulveda, J.O. Ighalo, A.U. Rajapaksha, L. Meili, Sewage sludge-derived biochar for the adsorptive removal of wastewater pollutants: a critical review. Environ. Pollut. **293**, 118581 (2022)

9. T. Getachew, A. Hussen, V.M. Rao, Defluoridation of water by activated carbon prepared from banana (Musa paradisiaca) peel and coffee (Coffea arabica) husk. Int. J. Environ. Sci. Technol. **12**(6), 1857–1866 (2015)

10. A. Dhillon, S.K. Soni, D. Kumar, Enhanced fluoride removal performance by Ce–Zn binary metal oxide: adsorption characteristics and mechanism. J. Fluorine Chem. **99**, 67–76 (2017)

11. M. Sarkar, D. Santra, Modeling fluoride adsorption on cerium-loaded cellulose bead-response surface methodology, equilibrium, and kinetic studies. Water Air Soil Pollut. **226**, 30 (2015)

12. R. Bhaumik, N.K. Mondal, S. Chattoraj, An optimization study for defluoridation from synthetic fluoride solution using scale of Indian major carp Catla (Catla catla): an unconventional biosorbent. J. Fluorine Chem. **195**, 57–69 (2017)

13. N. Mohammed, P. Palaniandy, F. Shaik, Pollutants removal from saline water by solar photocatalysis: a review of experimental and theoretical approaches. Int. J. Environ. Anal. Chem., 1–21 (2021)

14. N. Mohammed, P. Palaniandy, F. Shaik, Optimization of solar photocatalytic biodegradability of seawater using statistical modelling. J. Indian Chem. Soc. **98**, 100240 (2021)

15. M.H. Dehghani, R. Karri, E. Lima, *Green Technologies for the Defluoridation of Water*, Elsevier (2021)

16. K.K. Yadav, N. Gupta, V. Kumar, S.A. Khan, A. Kumar, A review of emerging adsorbents and current demand for defluoridation of water: bright future in water sustainability. Environ. Int. **111**, 80–108 (2018)

17. S. Joshi, S. Bajpai, S. Jana, Application of ANN and RSM on fluoride removal using chemically activated *D. sissoo* sawdust. Environ. Sci. Pollut. Res. **27**(15), 17717–17729 (2020)

18. R.H. Gumus, I. Okpeku, Production of activated carbon and characterization from snail shell waste (Helix pomatia). Adv. Chem. Eng. Sci. **5**(01), 51 (2014)

19. M. Regassa, F. Melak, W. Birke, E. Alemayehu, Defluoridation of water using natural and activated coal. Int. Adv. Res. J. Sci. Eng. Technol. **3**(1), 1–7 (2016)

20. G.V. Patankar, A.S. Tambe, B.D. Kulkarni, A. Malyshew, S.P. Kamble, Defluoridation of drinking water using PURAL® MG-20 mixed hydroxide adsorbent. Water Air Soil Pollut. **224**, 1727 (2013)

21. ISI, A. C. Powdered and Granular–Methods of sampling and its tests. Bureau of Indian Standards, IS, 877, New Delhi 1989

22. Standard Test Methods for Proximate Analysis of the Analysis Sample of Coal and Coke by Instrumental Procedures, A. S. T. M. Standard (1998)

23. Z.Y. Ping, L.X. Ya, L. Lu, C.F. Hua, Investigation of performances and mechanism of fluoride removal by Fe(Hl) loaded ligand exchange cotton cellulose adsorbent. Wuhan Univ. J. Nat. Sci. **10**, 936–940 (2005)

24. R.B. Baird, A.D. Eaton, E.W. Rice, L. Bridgewater, *Standard Methods for the Examination of Water and Wastewater*, Washington, DC: American Public Health Association, vol. 23, 2017.

25. P. Tripathi, V.C. Srivastava, A. Kumar, Optimization of an azo dye batch dsorption parameters using Box-Behnken design. Desalination **249**(3), 1273–1279 (2009)

26. M. Mourabet, A. El Rhilassi, H. El Boujaady, M. Bennani-Ziatni, R. El Hamri, A. Taitai, Removal of fluoride from aqueous solution by adsorption on Apatitic tricalcium phosphate using Box-Behnken design and desirability function. Appl. Surf. Sci. **258**(10), 4402–4410 (2012)

27. S. Joshi, S. Jana, Interaction of aqueous phase fluoride and Amberlite IR400Cl resin: evaluation of batch process. Chem. Data Collect. **32**, 100643 (2021)

28. A.A. Ayoola, F.K. Hymore, C.A. Omonhinmin, O.C. Olawole, O.S.I. Fayomi, D. Babatunde, O. Fagbiele, Analysis of waste groundnut oil biodiesel production using response surface methodology and artificial neural network. Chem. Data Collect. **22**, 100238 (2019)

29. R. Bhaumik, N.K. Mondal, Adsorption of fluoride from aqueous solution by a new low-cost adsorbent: thermally and chemically activated coconut fibre dust. Clean Technol. Environ. Policy **17**(8), 2157–2172 (2015)

30. S. Nehra, S. Raghav, D. Kumar, Biomaterial functionalized cerium anocomposite for removal of fluoride using central composite design optimization study. Environ. Pollut. **258**, 113773 (2020)

31. D. Nityanandi, C.V. Subbhuraam, Kinetics and thermodynamic of adsorption of chromium (VI) from aqueous solution using puresorbe. J. Hazard. Mater. **170**(2–3), 876–882 (2009)

32. A. Fakhri, Application of response surface methodology to optimize the process variables for fluoride ion removal using maghemite nanoparticles. J. Saudi Chem. Soc. **18**, 340–347 (2014)

33. G. Biswas, M. Kumari, K. Adhikari, S. Dutta, Application of response surface methodology for optimization of biosorption of fluoride from groundwater using Shorea robusta flower petal. Appl. Water Sci. **7**, 4673–4690 (2017)

34. M.K. Mondal, Removal of Pb (II) from aqueous solution by adsorption using activated tea waste. Korean J. Chem. Eng. **27**(1), 144–151 (2010)

35. B.D. Mistry, A Handbook of Spectroscopic Data-Chemistry (UV, IR, PRM, 13CNMR and Mass Spectroscopy), Oxford book company, Jaipur 2009.

36. K. Srividya, K. Mohanty, Biosorption of hexavalent chromium from aqueous solutions by Catlacatla scales: equilibrium and kinetics studies. Chem. Eng. J. **155**(3), 666–673 (2009)

37. A. Çelekli, S.S. Bireciklioglu, F. Geyik, H. Bozkurt, Prediction of removal efficiency of Lanaset Red G on walnut husk using

artificial neural network model. Bioresour. Technol. **103**, 64–70 (2012)

38. S.S. Tripathy, J.L. Bersillon, K. Gopal, Removal of fluoride from drinking water by adsorption onto alum-impregnated activated alumina. Sep. Purif. Technol. **50**, 310–317 (2006)